Noise effects on Padé approximants and conformal maps*

Ovidiu Costin¹, Gerald V Dunne^{2,**} and Max Meynig²

- Department of Mathematics, The Ohio State University, Columbus, OH 43210-1174, United States of America
- ² Department of Physics, University of Connecticut, Storrs, CT 06269-3046, United States of America

E-mail: gerald.dunne@uconn.edu

Received 18 July 2022; revised 19 October 2022 Accepted for publication 15 November 2022 Published 25 November 2022



Abstract

We analyze the properties of Padé and conformal map approximants for functions with branch points, in the situation where the expansion coefficients are only known with finite precision or are subject to noise. We prove that there is a universal scaling relation between the strength of the noise and the expansion order at which Padé or the conformal map breaks down. We illustrate this behavior with some physically relevant model test functions and with two nontrivial physical examples where the relevant Riemann surface has complicated structure.

Keywords: noise, Pade approximants, conformal maps, quantum field theory, Painleve

(Some figures may appear in colour only in the online journal)

1. Introduction

In physical and mathematical applications one frequently confronts the situation in which only a finite number of terms of an expansion of the function of interest are attainable, and also these coefficients may only be known to some finite precision. Padé approximants and conformal map approximants are well known tools for the first of these problems, as they provide analytic extrapolation of finite-order expansions of functions beyond their radius of convergence [1, 2]. They are powerful in applications, easy to use, and have an elegant physical and mathematical interpretation in terms of electrostatics [3–9]. In practice, however, their accuracy is affected not only by the *number* of original input coefficients, but also by the *precision* with which these

^{*} Dedicated to Michael Berry on the occasion of his 80th birthday, with sincere appreciation for a lifetime of profound and inspiring ideas and results, and also for his warmth, kindness and humour.

^{*} Author to whom any correspondence should be addressed.

coefficients are known. Here we ask the question: how does noisy input for a finite-order series affect the accuracy of Padé and conformal map approximants, for functions having a dominant branch point (or points)? This question has been studied previously for simple functions having a pole or poles [10–14], but in applications we are frequently interested in functions having branch points, and possibly quite complicated Riemann surface structure. In this case the effect of noise is much richer. We find that the approximation accuracy is determined by a universal relation between the strength of the noise and number of input terms, when the underlying function has branch points. We consider two different kinds of noise: (a) truncation of the coefficients at a fixed number of digits; (b) addition to the coefficients of uniform random noise of a chosen magnitude. The numerical results are consistent, and our mathematical analysis explains this observed universality.

We are motivated by two primary applications:

- (a) Padé approximation of a finite-order approximation of a *convergent* series, in order to probe near the dominant singularity(ies), to determine the location and nature of the branch point(s) (e.g. the *phase transition* point, the associated *critical exponent* and *Stokes constant*). This is a canonical problem, for example, in quantum field theory and statistical physics [15]. In a realistic physical application only finitely many expansion coefficients are available and their precision is typically limited.
- (b) Analytic extrapolation of a formal asymptotic expansion of a function, for which only a finite number of terms are known, and for which the coefficients are known imprecisely. This problem is regularized by a Borel transform, in which case it reduces to the first problem, in the Borel plane³. A more precise analytic continuation of the Borel transform leads to a more precise analytic continuation of the physical function (the inverse Borel transform) away from the region in which the original asymptotic expansion was generated.

Section 4 is devoted to the mathematical theory of noise sensitivity of Padé and conformal map methods, for which we prove rigorous results for a general class of functions. However, we also stress that there are simple practical applications of the underlying ideas in physical problems where little may be known in advance about the analytic properties of the function. This is particularly relevant for physical applications as it is frequently the case that the behavior of the function under study is dominated by a small number of singularities (either in the physical variable or in the Borel plane). Moreover, these singularities are typically point singularities of the form

$$f(p) \sim (\omega - \omega_0)^{\alpha} A(\omega) + B(\omega), \qquad \omega \to \omega_0$$
 (1)

where $A(\omega)$ and $B(\omega)$ are analytic at ω_0 . If this is in the physical plane, then we are most interested in extracting information about ω_0 , α and $A(\omega_0)$, which tell us the critical point, the critical exponent and the strength of the singularity. If this is the Borel transform, then ω_0 determines the strength of the leading non-perturbative effect, α determines the leading power-law correction, and $A(\omega)$ encodes the fluctuations about this leading non-perturbative contribution. For these cases, when the input coefficients are exactly known there is a precise relation between the accuracy of the analytic continuation and the *number* of input coefficients [16]. Here we extend these ideas to the situation where noise is included.

Our approach is guided by the electrostatic interpretation of Padé and its natural connection with conformal maps [3–9], a brief summary of which is given below in section 3. Think of

³ In this situation, in the absence of noise it can be shown that it is generically much more accurate to apply Padé to the Borel transform than to the original asymptotic expansion (recall that Padé is nonlinear so it does not commute with the transforms) [16].

the Padé poles as electrical charges in two dimensions, and consider the series expansion to be generated at $\omega=\infty$. Then, for a function with branch points, Padé arranges the charges so that (in the limit of an infinite number of input terms) they form a skeleton-like electrical conductor with end points at the branch points, and with flexible lines of charges (wires in the limit) that deform their shape and their intersection points such that the electrical (logarithmic) capacity is minimized. Roughly speaking, it is a one-dimensional analogue of the soap bubble problem. This perspective leads to several deep and useful results, which we use here to quantify the accuracy of a Padé approximation in the presence of noise.

The paper is organized as follows. In section 2 we present numerical evidence for the scaling laws governing the effects of noise on Padé and conformal map methods. Mostly based on existing results in the literature, section 3 makes the connection between Padé and conformal map approximants. Section 4 is devoted to the mathematical theory of noise sensitivity of Padé and conformal map methods, for which we prove rigorous results for a general class of functions. Section 5 discusses further physical and mathematical applications of our analysis. Our conclusions are summarized in section 6.

2. Numerical experiments of Padé 'breakdown'

Before coming to the general results in section 4, we provide some motivation based on numerical experiments which illustrate some of the key phenomena. Recall first that Padé approximants do not converge pointwise, but only *in capacity* [3–8] (see sections 3 and 4). This means that care is required in defining what we mean by 'breakdown' of the Padé approximation, and how we relate it to the number of input terms and the strength of the noise. Intuitively we certainly expect that if the coefficients become too noisy then the approximation will break down. In this paper we quantify this relationship.

At one level, the breakdown of Padé may be characterized by the appearance of spurious Padé poles which are not related to the actual singularities of the approximated function. For the case of rational functions, in the limit that the Padé order $N \to \infty$ these spurious poles appear on the unit circle with probability one [13, 14]⁴. For functions with branch points there is a richer structure of spurious poles [3, 17]. Here we introduce the concept of the breakdown order, and show that it is directly proportional to the logarithm of the noise strength.

2.1. Appearance of spurious Padé poles due to noise

We motivate our analysis with the following simple numerical experiment. The breakdown of Padé can be seen as a qualitative change in the distribution of Padé poles at a certain Padé order, in a way that is correlated with the strength of the noise. The noise causes the appearance of arcs of poles which form a natural boundary emanating from a genuine singularity. Consider mimicking the appearance of noise by truncating the input coefficients at a certain number of digits, and plot the Padé poles in the complex plane. See for example, figures 1 and 2, where we show the [n,n] Padé poles, obtained for a chosen truncation precision of the input coefficients, for the functions $(1+\omega)^{-1/9}$ and $(1+\omega^2)^{-1/9}$, respectively. We choose these representative functions recalling that the function $(1+\omega)^{\alpha}$ characterizes the leading local behavior near an isolated branch point, here normalized to be at $\omega = -1$, and it is also the Borel transform of the function with an asymptotic expansion $F(x) \sim \frac{1}{\Gamma(-\alpha)} \sum_{m=0}^{\infty} (-1)^m \Gamma(m-\alpha)/x^{m+1}$, which exhibits the generic Bender-Wu-Lipatov leading large order factorial growth typical of many

⁴ This has an interesting application to filtering noisy time-series [11, 12].

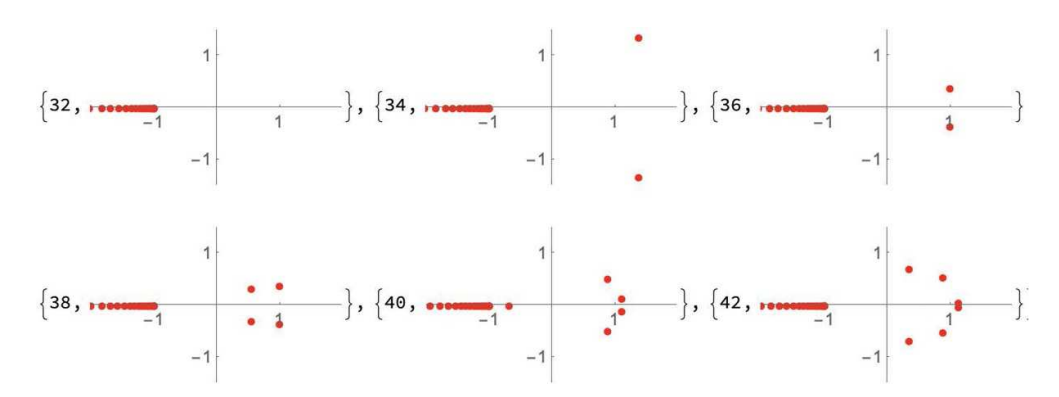


Figure 1. Padé poles for different orders, for the function $(1+\omega)^{-1/9}$, with coefficients truncated at 40 digit precision. Note that $\operatorname{Log}_{10}\left(4^{2\times33}\right)\approx40$. Spurious noise poles begin to appear at order 33, and in the limit they form as arcs originating at $\omega_{\inf}=+1$, the point of best approximation of Padé in the absence of noise. See figure 3.

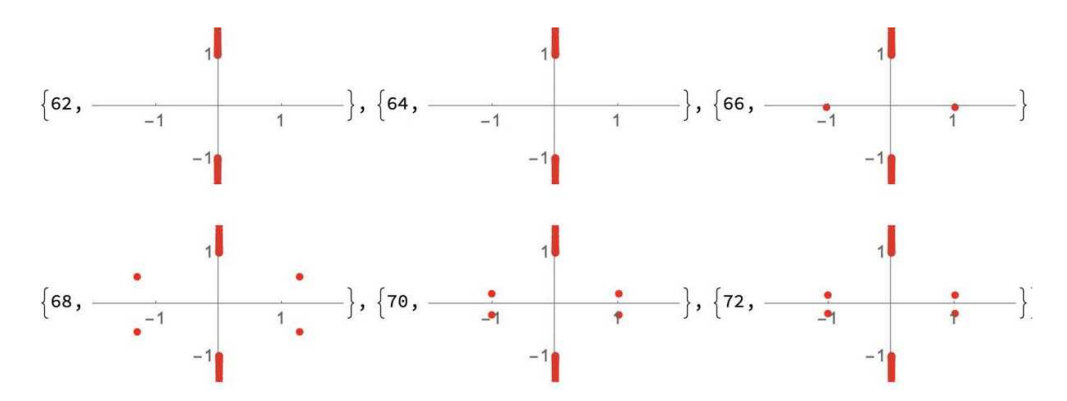


Figure 2. Padé poles for different orders, for the function $(1+\omega^2)^{-1/9}$, with coefficients truncated at 40 digit precision. Note that $\text{Log}_{10}\left(2^{2\times 66}\right)\approx 40$. Spurious noise poles begin to appear at order 66, and in the limit they form as arcs originating at $\omega_{\text{inf}}=\pm 1$, the points of best approximation of Padé in the absence of noise. See figure 4.

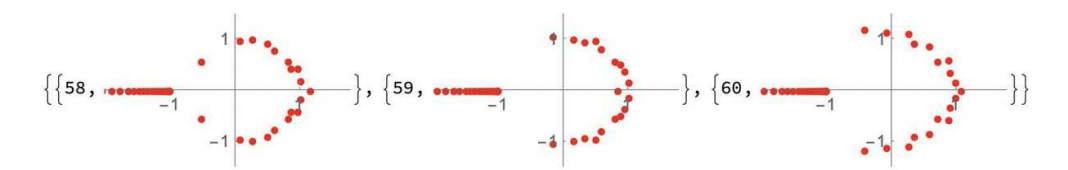


Figure 3. Padé poles for different orders, for the function $(1+\omega)^{-1/9}$, as in figure 1, but for larger orders, well beyond the order at which the Padé approximation breaks down. Observe that arcs of spurious noise poles are beginning to fill out near the unit circle, beginning with $\omega \approx +1$. This pattern formation is explained in section 4: see note 4.6.

applications in physics [18]. Similarly, the function $(1+\omega^2)^{\alpha}$ has two symmetric branch points, at $\omega=\pm i$. In both cases, we have rescaled the variable ω to place the singularity(ies) at distance 1 from the origin, thereby normalizing the radius of convergence to be 1.

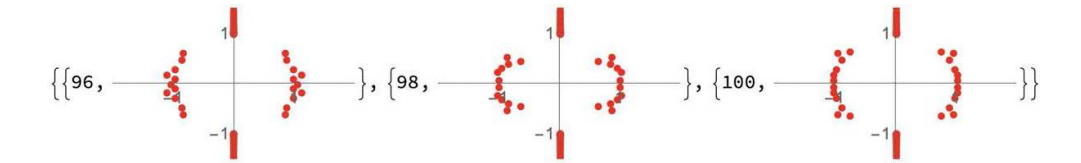


Figure 4. Padé poles for different orders, for the function $(1 + \omega^2)^{-1/9}$, as in figure 2, but for larger orders, well beyond the order at which the Padé approximation breaks down. Observe that arcs of spurious noise poles are beginning to fill out near the unit circle, beginning with $\omega \approx \pm 1$. This pattern formation is explained in section 4: see note 4.6.

As is well known, with the *exact* rational coefficients, Padé approximates the function $(1+\omega)^{-1/9}$ with a line of poles along the negative real axis, accumulating to the branch point at $\omega=-1$, while for $(1+\omega^2)^{-1/9}$ we find two lines of poles along the imaginary axis, coming in from $\pm i\infty$ and accumulating to the branch points at $\omega=\pm i$. These lines of poles are Padé's way of representing branch cuts for these functions⁵. However, when the input coefficients are truncated to a chosen number of digits, one finds that as we increase the number of input coefficients, at a certain order Padé begins to produce spurious 'noise poles', which form arcs in the complex plane. From this numerical experiment we make two important observations:

- (a) The Padé order at which these noise poles begin to appear is correlated with the chosen digit truncation order of the input coefficients. See figures 1 and 2. With the chosen digit truncation order of 40, the Padé order at which the noise poles begin to appear is approximately given by $N_c = 33 \approx 40/(2\log_{10}(4))$ for $(1+\omega)^{-1/9}$, and by $N_c = 66 \approx 40/(2\log_{10}(2))$ for $(1+\omega^2)^{-1/9}$. The factor of 2 difference between N_c for these two cases is a first hint towards a more general result, as it corresponds to the difference in the logarithmic capacities for the Riemann surfaces of these two functions. For an explanation of the origin of these logarithmic estimates, see section 3.2 below.
- (b) The formation of spurious noise poles for more general functions is explained in section 4. There we also explain the structure of the arcs of noise poles, in the large N limit. As the truncation errors become larger, the noise poles form arcs, expanding from special points ω_{\inf} on the circle of convergence in Ω (recall we have normalized this to be the unit circle $\omega \in S^1$). Roughly speaking, these special points ω_{\inf} are the points on the circle of convergence most distant from the actual singularities. These are also the points on S^1 where, without noise, the Padé extrapolation is the most accurate. For example, for the function $(1+\omega)^{-1/9}$, we have $\omega_{\inf} = \pm 1$. Compare with figures 1 and 2. These ω_{\inf} points are define precisely below in theorem 4.4: they are the point(s) at which Padé (without noise) is most accurate. In the large N limit these noise poles form a circle of poles representing the natural boundary of the noise function.

2.2. Capacity in the presence of noise

In the electrostatic formulation of Padé approximation (in the absence of noise), the logarithmic capacity is an important quantity in determining the accuracy, especially close to the

⁵ In fact, interlaced with Padé zeros. Recall that since Padé produces a rational function, it only has poles and zeros.

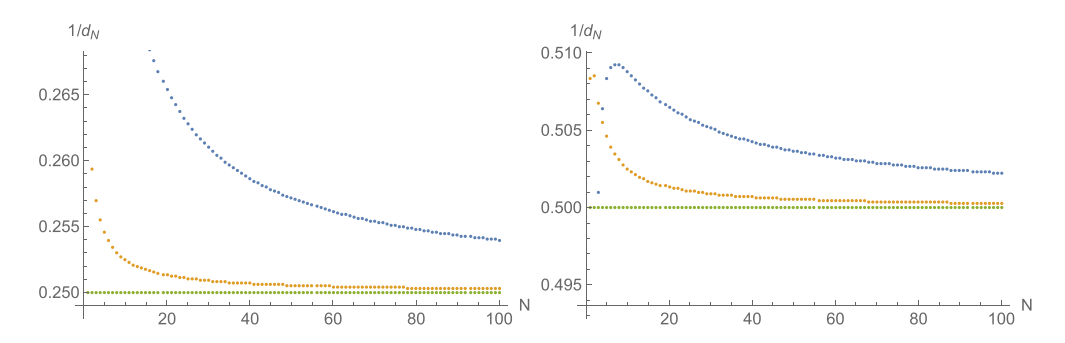


Figure 5. Plots of the convergence of $1/d_N(f)$, defined in (2), to the capacity, for the functions $f(\omega) = (1+\omega)^{-1/9}$ (left) and $f(\omega) = (1+\omega^2)^{-1/9}$ (right), showing convergence to the exact values (in green) 1/4 and 1/2, respectively. The blue dots are $1/d_N(f)$, and the orange dots show a second order Richardson acceleration.

point of expansion [3–5]. In this section we explore the connection between capacity and noise sensitivity. The capacity can be estimated from the Padé poles as follows. Let $\{\omega_i\}_{i=0}^N$ be the set of poles of the diagonal [N,N] Padé approximant of the function $f(\omega)$. In the large N limit, the ω_i accumulate along a set $\mathcal C$ of branch cuts such that f is single-valued in $\mathbb C\setminus \mathcal C$ (clearly, rational approximants such as Padé can only converge in domains of single-valuedness of f). Construct the following quantity

$$d_N(f) := \left(\prod_{1 \leqslant j < i \leqslant N} |\omega_i - \omega_j|\right)^{\frac{2}{N(N-1)}}.$$
 (2)

In the $N \to \infty$ limit, $d_N(f)$ approximates the reciprocal of the logarithmic capacity of C, [4]:

$$\lim_{N \to \infty} d_N(f) = \frac{1}{c}.$$
 (3)

The logarithmic capacity is also known as the 'transfinite diameter' and the 'Chebyshev constant', and can be computed in a variety of relatively simple ways [4, 19–21] and, in symmetric cases, based on continued fraction representations of Padé, [22]. Figure 5 shows the convergence of $d_N(f)$ to the known capacity values of $\frac{1}{4}$ and $\frac{1}{2}$, respectively, for the one-cut and two-cut functions $(1+\omega)^{-1/9}$ and $(1+\omega^2)^{-1/9}$ discussed in the previous section. An important result of Stahl [3] is that in the family of all possible cuts $\mathcal C$ such that f is single-valued in $\mathbb C\setminus\mathcal C$, the logarithmic capacity c of the set $\mathcal C$ is minimal. It is shown in [3] that this minimal c equals $\psi'(0)$, where $\psi(\omega)$ is the conformal map from $\mathbb C\setminus\mathcal C$ to $\mathbb D$, normalized so that $\psi'(0) > 0$. By domain monotonicity, c < 1, see [23].

Now let us introduce noise to the coefficients, by adding to the original truncated series a series with random coefficients:

$$f(\omega) := \sum_{k=0}^{m} f_k \omega^k \to f_{\epsilon}(\omega) := f(\omega) + \mathcal{N}_{\epsilon}(\omega); \ \mathcal{N}_{\epsilon}(\omega) := \epsilon \sum_{k=0}^{m} r_k \omega^k. \tag{4}$$

Here r_k are independent random variables distributed uniformly in [-1,1], and $0 < \epsilon < 1$ is a constant that characterizes the strength of the noise. Such a noise function, $\mathcal{N}_{\epsilon}(\omega)$, would model settings in which the Maclaurin coefficients f_k are available in floating point arithmetic with a fixed number of digits. We now apply a Padé approximant to the noisy truncated expansion $f_{\epsilon}(\omega)$ and analyze the distribution of the resulting poles. We average over many

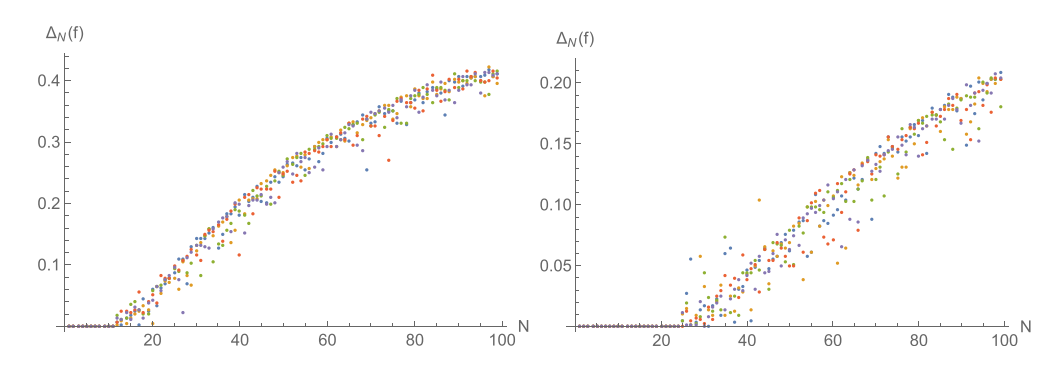


Figure 6. Plots of the deviation in the capacity due to noise, $\Delta_N(f_\epsilon)$, defined in (5), for the one-cut and two-cut functions $(1+\omega)^{-1/9}$ and $(1+\omega^2)^{-1/9}$. The different colored dots correspond to five different realizations of the random noise in (4), all with a chosen noise strength $\epsilon=10^{-20}$. We see a clear breakdown once a certain truncation order N is reached, and we observe that this truncation order is twice as large for the two-cut function.

realizations of the random noise. The presence of the noise function eventually introduces new singularities in the perturbed function, which has the effect of augmenting the capacitor \mathcal{C} and increasing the corresponding capacity c. With this introduction of noise, one finds that the convergence to the true capacity of the function, shown in figure 5, breaks down at a certain order that is correlated with \mathcal{C} in a way that is calculated in section 4.

This can be seen by considering the deviation from the noise-free case⁶

$$\Delta_N(f_{\epsilon}) := \left| d_N(f_{\epsilon})^{-1} - d_N(f_{\epsilon'})^{-1} \right|. \tag{5}$$

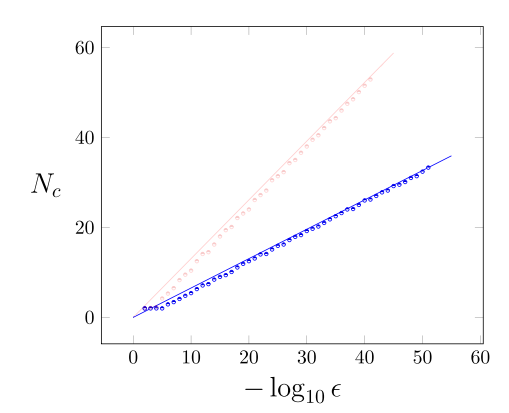
Plotting this deviation $\Delta_N(f)$ as a function of the truncation order parameter N, we observe a clear kink-like transition occurring at a certain order. See figure 6. One can therefore estimate the breakdown point of Padé as the location of this sudden kink transition. In practice, we fix a value for the noise strength ϵ , and calculate the smallest N such that $\Delta_N(f_{\epsilon}) > \delta$, with δ a chosen acceptable precision threshold. In our analysis here we have chosen the error threshold $\delta = 10^{-3}$.

We can adopt the order at which this kink transition occurs (averaged over multiple realizations of the noise ϵ) as a definition of the critical order N_c at which Padé breaks down. With this definition, we can analyze the dependence of N_c on the noise strength ϵ in (4). This is shown in figure 7 for the one-cut function $(1+\omega)^{-1/9}$ and the two-cut function $(1+\omega^2)^{-1/9}$. We see a definite linear behavior in this log plot, and note that the slope in the two cases differs by a factor of 2. This matches the factor of 2 observed in the numerical experiments in section 2.1 and in figure 6. These numerical experiments, also repeated with other functions having different capacities, suggest a scaling relation of the form

$$N_{\rm c} = ({\rm constant}) \times \frac{\log_{10}(\epsilon)}{\log_{10}(c)}$$
 (6)

where ϵ is the noise strength and c is the capacity (recall that c < 1). The overall constant factor appears to be universal, with an approximate value of 0.4. In order to explain why this is the

⁶ Here $\epsilon' = \epsilon 10^{-100}$ is a noise level small enough to have negligible impact but still to improve the computation time.



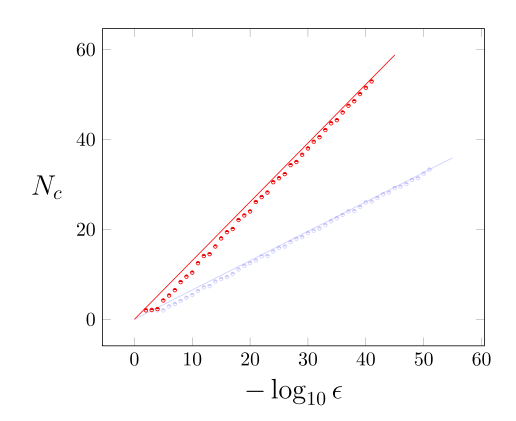


Figure 7. Plots of the Padé breakdown order N_c , as defined in the text, for the model functions $(1+\omega)^{-1/9}$ (left, blue dots) and $(1+\omega^2)^{-1/9}$ (right, red dots). Note that N_c is linear in the log of the noise strength ϵ , as in (6). The faint shadow lines indicate the plot for the other function, to emphasize that the slope differs by a factor of 2 in the two cases. The slope scales with the log of the capacity, as in (6).

case, and to prove general results, we turn now to a more detailed discussion of the relation of Padé to conformal maps, which provides a more analytic approach to this problem.

3. Padé and conformal maps

The relation between Padé approximants and conformal maps follows from the remarkable and intuitively useful physical interpretation of Padé in terms of two-dimensional electrostatics, known as logarithmic potential theory [3–6]. Two dimensional electrostatic potentials are harmonic functions, for which conformal maps are of course a natural tool [24]. We briefly review the relevant ideas and results. For excellent reviews see [4–6].

The convergence of near-diagonal Padé approximants to functions with branch points is a rich subject, elucidated in the fundamental paper of Stahl [3]. It is interesting to note that convergence in capacity is established at this time only for functions analytic on $\Omega(\mathbb{C} \setminus E)$, for sets E of zero logarithmic capacity or in domains in \mathbb{C} bounded by piecewise analytic arcs under a stringent symmetry condition [3]. The first class of functions is the relevant one here. For further developments and refinements, see [7, 8].

3.1. Potential theory and physical interpretation of Padé approximants

Given a function $f(\omega)$ with branch points in \mathbb{C} , let \mathcal{D}' be any domain of single-valuedness of f, and let $E' = \partial \mathcal{D}'$ be its boundary. If the function f has finitely many singularities, $\partial \mathcal{D}'$ is a set of piecewise analytic arcs joining branch points of f, and some accessory points (similar to those of the Schwarz–Christoffel formula) associated with junctions of these analytic arcs. So E' is the union of the chosen set of branch cuts for f.

Now think of E' as an electrical conductor on which we place a unit charge. The electrostatic potential on a conductor is constant, and we normalize so that the potential vanishes on E': V(E') = 0. Therefore the electrostatic capacitance of E' is $cap(E') = 1/V(\infty)$. In two

dimensions the potential energy per particle of a system of charges placed at the locations $E = \{\omega_i\}_{1 \le i \le N}$ is:

$$\mathcal{E}_N(E) = -\sum_{1 \leqslant i < j \leqslant N} \log |\omega_i - \omega_j| =: -\frac{N(N-1)}{2} \log d_N(E). \tag{7}$$

The minimal potential energy is attained with the charges at the equilibrium positions, known as Fekete points [4]. In the limit $N \to \infty$, $d_N(E)$ gives the harmonic capacity, the exponential of the usual capacity with respect to infinity. Compare with (2). The key relations to Padé are as follows:

- (a) The electrostatic minimization process results in the *minimal capacitor*, and asymptotically it coincides with the pole locus of Padé (where the Padé is constructed from an expansion about infinity rather than about zero, in order to match the electrostatic interpretation). In other words, in the $N \to \infty$ limit the Padé poles are placed along an electrical conductor E, which is essentially the set of branch cuts chosen by Padé, and the complement \mathcal{D} of E is the domain of convergence of Padé [3].
- (b) For $\omega \in \mathcal{D}$, the Green's function is related to the potential as $|G_{\mathcal{D}}(\omega)| = e^{-V(\omega)}$. In fact, if \mathcal{D} is simply connected, $|G_{\mathcal{D}}(\omega)| = \psi_{\mathcal{D},\infty}(\omega)$, where $\psi_{\mathcal{D},\infty}$ is the conformal map from \mathcal{D} to the unit disk \mathbb{D} , seen from infinity with $\psi_{\mathcal{D},\infty}(\infty) = 0$ ([3]). This conformal map can be recovered, in the limit $N \to \infty$, from the harmonic function $|G_{\mathcal{D}}|$, see proposition 3.1 below. Summarizing for diagonal Padé from theorem 1 by Stahl [3],
 - 1. For any $\epsilon > 0$ and any compact set $V \subset \mathcal{D} \setminus \{\infty\}$ we have

$$\lim_{N \to \infty} \operatorname{cap}\{\omega \in V | (f - [N, N]_f)(\omega) > (G_{\mathcal{D}}(\omega) + \epsilon)^{2N} \} = 0$$
 (8)

2. If f has branch points, which occurs if $G_{\mathcal{D}} \neq 0$, then for any compact set $V \subset \mathcal{D} \setminus \{\infty\}$ and any $0 < \epsilon \leqslant \inf_{\omega \in V} G_{\mathcal{D}}(\omega)$ we have

$$\lim_{N \to \infty} \operatorname{cap}\{\omega \in V | (f - [N, N]_f)(\omega) < (G_{\mathcal{D}}(\omega) - \epsilon)^{2N}\} = 0.$$
 (9)

- (c) In this sense, Padé effectively 'creates its own conformal map' and its own domain \mathcal{D} . Geometrically, join all the branch points of f by a perfectly conducting, connected, infinitely flexible wire W in such a way that the function f is single-valued in the complement of W. The wire generically has further junction nodes besides the branch points. Deform the wire until the capacitance of the final, extremal, wire E with respect to infinity is minimized.
- (d) The equilibrium measure μ on E is the equilibrium density of charges on E. As $N \to \infty$, the poles of the near diagonal Padé approximants place themselves (except for a set of zero capacity) close to E, and Dirac masses placed at these poles converge in measure to μ [3].
- (e) The numerators and denominators of Padé approximants are orthogonal polynomials, in a generalized sense, along arcs in the complex domain, but therefore without a bona-fide Hilbert space structure. According to [3], this is the ultimate source of capacity-only convergence, and of the appearance of spurious poles. Spurious poles can be eliminated, see [3], p 145, (8), after which convergence is uniform.

Proposition 3.1. Assume that spurious poles have been eliminated and convergence is uniform [3] in a simply connected domain \mathcal{D} . Let f be analytic in the unit disk and have branch points in \mathbb{C} . Then, for large N and $\omega \in \mathcal{D}$,

$$|f(\omega) - [N,N]_f(\omega)|^{1/2N} = |\psi(\omega)|(1+o(1))$$
 (10)

where ψ is the conformal map from the domain of analyticity of the Padé approximants to \mathbb{D} . In fact, with an appropriate choice of branch,

$$e^{-i\lambda} (f(\omega) - [N, N]_f(\omega))^{1/2N} = \psi(\omega)(1 + o(1))$$
 (11)

for some phase $e^{-i\lambda}$.

Proof. Choose a disk $D \subseteq \mathbb{D}$ around the origin. Since ψ is conformal and $\psi(0) = 0$, we have $\psi(z) \neq 0$ on ∂D . Let $\kappa = \max_{\partial D} |\psi| (\min_{\partial D} |\psi|)^{-1}$. Note also that, inside \mathcal{D} we have $|\psi| < 1$. Choose a $\delta > 0$ small enough so that on ∂D we have $|\psi|(1+\delta) < 1$. Let $\epsilon = \kappa \delta$. Fixing a radius R, combining (8) and (9) we get for that for large N (10) holds on ∂D . By the maximum principle, the inequality holds in D. For the second part, we note that $|\psi|$ is harmonic, and $|f - [N, N]_f| = |\psi|^{2N} (1 + o(1))$, while $(f(\omega) - [N, N]_f(\omega))$ is analytic⁷.

3.2. Padé and conformal maps in the presence of noise: two simple examples

An important consequence of these results connecting Padé with logarithmic potential theory and conformal map methods is that we can now understand how and why noise affects a Padé approximant: in the large *N* limit the noisy input coefficients effectively propagate through the Padé algorithm by composition of the conformal map with the original (noisy) series. Therefore the problem can be re-cast as the analysis of the effect of a conformal map on a noisy series, and this can be quantified precisely, providing us with a sharp quantitative estimate of the relation between the noise and the number of terms before Padé breaks down.

It is instructive to show how this works for the generic case of a function with one dominant branch point, which we can normalize to be at $\omega = -1$. Then in the large N limit the effect of noise on the Padé approximant is given by composition of the truncated noisy series $f_{\epsilon}(\omega)$ in (4) with the one-cut conformal map:

$$\omega = \frac{4z}{(1-z)^2} =: \varphi(z) \quad \longleftrightarrow \quad z = \frac{\sqrt{1+\omega}-1}{\sqrt{1+\omega}+1} =: \psi(\omega)$$
 (12)

which maps the cut ω plane to the interior of the unit disk in the conformal z plane. This maps the branch point $\omega = -1$ to z = -1, the origin $\omega = 0$ to z = 0, and the upper (lower) edge of the cut $\omega \in (-\infty, -1]$ is mapped to the upper (lower) half of the unit circle |z| = 1. Therefore

$$\left(\frac{4z}{(1-z)^2}\right)^m = 4^m \sum_{k=0}^{\infty} z^{m+k} \binom{k+2m-1}{k}$$
 (13)

and so the composition yields:

$$(f_{\epsilon} \circ \varphi)(z) = \sum_{m=0}^{\infty} 4^m \sum_{k=0}^{\infty} (a_m + \epsilon r_m) \left(\frac{4z}{(1-z)^2}\right)^m$$
$$= \sum_{m=0}^{\infty} z^m \sum_{k=0}^{m} (a_k + \epsilon r_k) 4^k \binom{m+k-1}{m-k}.$$
 (14)

The variance of $[z^m](f_{\epsilon} \circ \varphi)(z)$, the coefficient of z^m , is

$$\sigma^{2}(m) = \langle ([z^{m}](f_{\epsilon} \circ \varphi)(z) - \langle [z^{m}](f_{\epsilon} \circ \varphi)(z) \rangle)^{2} \rangle. \tag{15}$$

⁷ Our results extend to near-diagonal Padé approximants which, together with the diagonal ones, are the most relevant in applications.

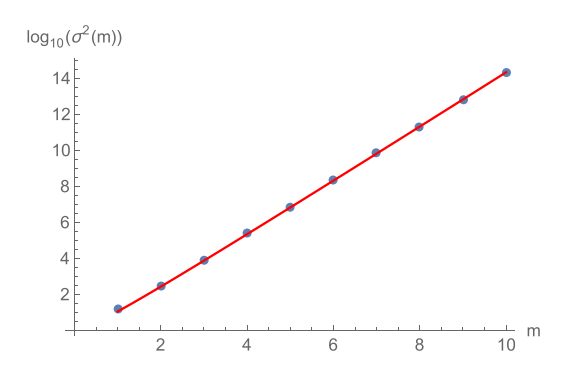


Figure 8. A log plot of $\sigma^2(m)$ in (16) (blue dots) compared with the Euler–Maclaurin leading large m approximation in (17). For this comparison plot we have suppressed the unimportant common overall $\frac{\epsilon^2}{3}$ factor in (16) and (17).

Because the random noise averages to zero, $\langle r_m \rangle = 0$, the variance reduces to

$$\sigma^{2}(m) = \epsilon^{2} \left\langle \left(\sum_{k=0}^{m} r_{k} 4^{k} \binom{m+k-1}{m-k} \right)^{2} \right\rangle$$

$$= \frac{\epsilon^{2}}{3} \sum_{k=0}^{m} 4^{2k} \binom{m+k-1}{m-k}^{2}.$$
(16)

At large m, the summand is strongly peaked around $k \approx \frac{m}{\sqrt{2}}$, and so the sum can be evaluated by a straightforward Euler–Maclaurin analysis. We find the large m estimate

$$\sigma^{2}(m) \approx \frac{\epsilon^{2}}{3} \frac{\left(\sqrt{2}+1\right)^{4m}}{2^{1/4}\sqrt{2\pi m}} \left(1+o\left(\frac{1}{m}\right)\right) \tag{17}$$

which is in excellent agreement with the variance in (16) even at modest values of m: see figure 8.

To connect back to the Padé approximant, recall that for a diagonal [N, N] Padé approximant, the original series is expanded to order m = 2N, and the optimal truncation of the re-expansion after the conformal map is to truncate the z expansion also at this order [23]. Therefore, in the variance we identify m = 2N. We arrive at a sharp estimate for the slope in the empirical identification (6),

$$N_c \approx \frac{-\log_{10}(\epsilon)}{4\log_{10}\left(1+\sqrt{2}\right)}. (18)$$

The corresponding conformal map with M symmetrically placed radial cuts emanating to infinity from branch points at $\omega^M = -1$ is [23, 25] (with the natural branch choices):

$$\omega = \frac{2^{2/M}z}{(1-z^M)^{2/M}} =: \varphi_M(z) \quad \longleftrightarrow \quad z = \sqrt[M]{\frac{\sqrt{1+\omega^M}-1}{\sqrt{1+\omega^M}+1}} =: \psi_M(\omega). \tag{19}$$

The analysis is therefore identical, with ω replaced by ω^M and z replaced by z^M , so the only real difference is the scaling of the highest term in the expansion. We therefore find

$$N_{\rm c} \approx \frac{-M\log_{10}(\epsilon)}{4\log_{10}\left(1+\sqrt{2}\right)}. (20)$$

This agrees with the scaling factor of 2 difference between the one-cut and two-cut cases found in sections 2.1 and 2.2.

Recalling that for this symmetric configuration of M radial cuts, the capacity is $c_M = \psi_M'(0) = 4^{-1/M}$ [9, 23], we can re-express (20) in a more suggestive form:

$$N_{\rm c}(M) = \frac{\log_{10}(\sqrt{2})}{\log_{10}(1+\sqrt{2})} \frac{\log_{10}(\epsilon)}{\log_{10}(c_M)} \approx (0.3932...) \frac{\log_{10}(\epsilon)}{\log_{10}(c_M)}$$
(21)

This agrees very well with the numerical fit of ≈ 0.4 of the slope in (6), for the data in the numerical experiments shown in figure 7, and it incorporates the correct scaling with the capacity.

4. General mathematical theory of the effect of noise on Padé and conformal maps

In this section we summarize a number of precise mathematical results showing universality in the breakdown of conformal map methods and of Padé approximations. The relevant proofs will be the subject of a separate technical paper. These results explain the observations arising from the numerical experiments in section 2.1, and also explain and generalize the quantitative results in section 3.

Padé and conformal maps are related due to the key result of Stahl [3], described above in (8)–(9). This has the remarkable consequence that at large order, the leading error of Padé is expressed solely in terms of the conformal map $\psi(\omega)$ and its inverse $\varphi(z)$, not in terms of the function $f(\omega)$. As in the case of conformal map methods, this dramatically simplifies the problem, as we can decouple the analysis from the (unknown) function f and concentrate on a conformal map common to functions with the same singularity structure. The introduction of noise reduces the accuracy of Padé and conformal map methods, by various natural measures of accuracy listed in the definition 4.1 below. The general mathematical theory for estimating the accuracy is naturally phrased in terms of the relevant conformal maps.

4.1. Notation and mathematical framework

Let $\mathcal D$ be a simply connected domain, more generally a Riemann surface Ω , in which the function of interest, $f \colon \Omega \to \mathbb C$, is analytic. We denote by $\psi = \psi(\omega)$ the conformal map, or more generally the uniformization map, from Ω to $\mathbb D$, and $\varphi = \varphi(z)$ its inverse. We normalize such that the leading singularity of f is at $\omega_0 = 1$, and so f is analytic in the unit disk $\mathbb D$ and on Ω , and we write

$$f(\omega) = \sum_{j=0}^{\infty} f_j \omega^j.$$
 (22)

We denote by $[N,N]_f$ the diagonal Padé approximant P_N/Q_N of f. Here P_N,Q_N are defined as usual to be the unique pair of polynomials of degree N normalized so that the coefficient of ω^N in P_N is 1, and such that the Maclaurin coefficients of order up to and including 2N of $[N,N]_f$

agree with those of f [1, 2]. For a function g we denote by $g_{[m]}$ its Maclaurin polynomial of order m.

We write the expansion of the inverse map $\varphi(z)$ as a Taylor series,

$$\varphi(z) = \sum_{k=1}^{\infty} b_k z^k \tag{23}$$

to emphasize the composition with the conformal map. Noting that $\varphi(\mathbb{D}) = \Omega$, and that f is analytic in Ω , it follows that the composition $f \circ \varphi$ is analytic in \mathbb{D} . Hence the series of $f \circ \varphi$,

$$(f \circ \varphi)(z) = \sum_{j=0}^{\infty} f_j \varphi^j(z) := \sum_{k=0}^{\infty} c_k z^k$$
 (24)

converges in the unit disk \mathbb{D} . Let r_i be independent random variables as in section 2.2, let $\Omega \supset \mathbb{D} \neq \mathbb{C}$ be a simply connected domain in \mathbb{C} or more generally a Riemann surface containing the unit disk \mathbb{D} on its first Riemann sheet. We assume that only finitely many singular points, $\mathcal{B} = \{\omega_1, \dots, \omega_M\}$, lie on the unit circle and the boundary $\partial\Omega$ of the Riemann surface.

Let $\psi:\Omega\to\mathbb{D}$ be the conformal or uniformization map of Ω to \mathbb{D} and $\varphi=\psi^{-1}$. Let \mathfrak{b} be the image of the circle S^1 in Ω through ψ , $\mathfrak{b}:=\{z:|\varphi(z)|=1\}=\psi(S^1)$. It is a piecewise analytic curve whose nonanalytic points are $\psi(\omega_i), i=1,\ldots,M$. Let $z_{\inf}\in\mathfrak{b}$ be such that $|z_{\inf}|=\min_{z\in\mathfrak{b}}|z|$. It is a simple result in conformal representations that $|z_{\inf}|<1$.

The effect of noise on Padé reduces to the effect of noise on composition with a conformal map as discussed in the following.

Definition 4.1. In reconstructing f from its truncated expansion $f_{[m]}$ by using a conformal map or relatedly, by Padé, both using $f \approx (f \circ \varphi)_{[k]} \circ \psi$, $k \ge n$, the noise-induced breakdown of approximation can be defined in a number of ways:

- (a) The first value of k for which the coefficient c_k in (24) becomes inaccurate (by some chosen measure of accuracy).
- (b) The first value of k for which there is a $z \in \mathbb{D}$ for which the approximation $(f \circ \varphi)(z) \approx (f \circ \varphi)_{[k]}(z)$ becomes inaccurate.
- (c) For a fixed $z \in \mathbb{D}$, the first value of k for which the approximation $(f \circ \varphi)(z) \approx (f \circ \varphi)_{[k]}(z)$ becomes inaccurate.

As we will see, (a) and (b) above are roughly equivalent, while (c) provides more local information.

We quantify the loss of accuracy in corollary 4.3 and, much more sharply, in theorem 4.4 below. These are generalizations of the results derived in section 3.2 for the simple representative conformal maps for functions with one branch cut, or a symmetric set of radial branch cuts. This analysis shows that in general the important mathematical object is the conformal map, either the explicit one being used, or the one that Padé effectively constructs (recall the discussion of the electrostatic interpretation of Padé in section 3.1).

Note 4.2.

(a) Since $[N,N]_f$ has the same Maclaurin coefficients as f up to and including order 2N, for any φ , the composition maps $(f \circ \varphi)$ and $([N,N]_f \circ \varphi)$ have the same Maclaurin coefficients up to and including the 2Nth order.

- (b) Assume that spurious poles have been eliminated from the Padé approximant [3]. In [23] it is shown that the accuracy of approximation of $[N,N]_f$ is lower than, and of the same order of magnitude as, that of $(f \circ \varphi)_{[2N]}$.
- (c) The approximation provided by Padé is that of $(f \circ \varphi)_{[2N]} + \sum_{k \geqslant 2N+1} a_k z^k$, where the a_k are generally different from the Maclaurin coefficients of $(f \circ \varphi)$ and make Padé less accurate than $(f \circ \varphi)_{[2N]}$. By any sensible measure of accuracy, Padé breaks down earlier than the associated conformal map, albeit not significantly earlier.

The following result characterizes the behavior of Pade approximants when noise becomes dominant and explains the observed appearance of a circle of poles surrounding the point of expansion. See section 4.1 for the concepts and notations used.

Proposition 4.3. Let \mathcal{N}_{ϵ} be the noise function introduced in (4), and let n(z) be the large m limit of the composition of this noise function with φ :

$$n(z) := (\mathcal{N}_{\epsilon} \circ \varphi)(z) = \sum_{k=0}^{\infty} n_k z^k.$$
 (25)

Then

- (a) The unit circle S^1 in Ω is a natural boundary of \mathcal{N}_{ϵ} , and \mathfrak{b} is a natural boundary of $\mathcal{N}_{\epsilon} \circ \varphi$.
- (b) For each realization of the noise variables r_i we have, with probability one,

$$\limsup_{k} |n_k|^{\frac{1}{k}} = |z_{\inf}|^{-1} \quad where \quad |z_{\inf}| = |\psi(\omega_{\inf})| := \inf_{\omega \in S^1} |\psi(\omega)|$$
 (26)

See Note 4.6 below for an intuitive explanation and further comments.

There is in fact the following sharper result. We write $z_{\text{inf}} = \psi(\omega_{\text{inf}})$, for one or more ω_{inf} , and we write ω_{inf} as a phase: $\omega_{\text{inf}} = e^{i\theta_{\text{inf}}}$. For the result we assume the generic condition $\alpha = \left(\frac{\psi''}{\psi} - \left(\frac{\psi'}{\psi}\right)^2\right)(\theta_{\text{inf}}) \neq 0$. (Note that, by conformality, $\psi' \neq 0$.).

Theorem 4.4. For large k, n_k is a random variable of zero average and standard deviation

$$\sigma(n_k) = A \epsilon k^{-\frac{1}{4}} |z_{\text{inf}}|^{-k} (1 + o(1))$$
(27)

where

$$A = 3^{-\frac{1}{2}} (2\pi)^{\frac{3}{4}} |\psi'(\omega_{\inf})| [\Re \alpha(\omega_{\inf})]^{-\frac{1}{4}}.$$

Corollary 4.5. For a given error threshold δ ,

(a) The breakdown condition on the coefficient n_k is

$$A \epsilon k^{-1/4} |z_{\inf}|^{-k} (1 + o(1)) \gtrsim \delta.$$

$$(28)$$

(b) The condition of breakdown of approximation at $\omega = \varphi(z)$, $|\omega| > 1$, is

$$A \epsilon k^{-1/4} \left| \frac{z}{z_{\inf}} \right|^k \left| \frac{1}{1 - z_{\inf}/z} \right| \gtrsim \delta$$
 (29)

(where $|\omega| > 1$ implies $|z| > |z_{\text{inf}}|$).

In the limiting case |z| = 1, (b) reduces, up to a constant, to the condition in (a).

Note 4.6.

- (a) Since it is a function with O(1) random coefficients, \mathcal{N}_{ϵ} is analytic in $\mathbb{D} \subset \Omega$, and the unit circle $S^1 \subset \Omega$ is, with probability one, a natural boundary [26] of \mathcal{N}_{ϵ} . The circle of singularities begins making its mark on the series extrapolation when the noise in the coefficients becomes significant. Intuitively, extrapolation quality relies on cancellation of coefficients, and hence the points of best extrapolation accuracy are also those which are most sensitive to noise. That is where the effects of the noise first appear. Thereafter, noise poles spread out on a circle in the 'order' of approximation quality. Hence the circle of noise poles starts at the 'best' point on S^1 , and grows from there until it covers the whole of S^1 .
- (b) This result explains the pattern of spurious poles in figures 1 and 2. The spurious poles form arcs near the points ω_{inf} , which in figure 1 is the point $\omega_{inf} = \pm 1$, and in figure 2 are the two points $\omega_{inf} = \pm 1$. Figures 3 and 4 show the arcs of noise poles well beyond the breakdown order, where we see the noisy circular arcs forming, beginning at the relevant value(s) of ω_{inf} .

Note 4.7.

- (a) Padé provides an efficient method to estimate the key quantity z_{inf} in proposition 4.3, even with only a limited number of input coefficients: one simply computes the difference $[N,N]_f(\omega) [N-1,N-1]_f(\omega)$, for $\omega \in \partial \mathbb{D}$ and looks for the smallest value.
- (b) For Padé, one could also estimate z_{inf} empirically, with high accuracy, as follows. One constructs a known function g with branch points at the tips of \mathcal{D} and analytic in \mathcal{D} , calculates Padé approximants of sufficient order for g, and measures the error of approximation along the unit disk in ω . Then z_{inf} follows from (10) above.
- (c) It follows from the same analysis that the region where conformal map or Padé approximants are guaranteed to be insensitive to noise is the unit disk in Ω , the same as the domain of convergence of the original series. Any extrapolation beyond this domain of convergence is eventually affected by noise.
- (d) For diagonal [N, N] Padé we identify m = 2N and we therefore have a general mathematical characterization of breakdown, expressed in a form analogous to (6) and (21):

$$N_c^{\inf} = \frac{\log_{10}(\epsilon)}{2\log_{10}(z^{\inf})}.$$
 (30)

Thus, the proportionality factor is most naturally identified with z_{inf} , which is a property of the conformal map associated with Padé. Importantly, it does not depend on knowing the function f, but just the locations of its singularities. In practical applications, even approximate information about the *leading* singularities of f can be used to obtain good approximations to N_c^{inf} , as shown in several examples in the next section.

(e) Note that for the configurations of M symmetric branch points, discussed in section 3.2, which are often relevant in physical applications, this general breakdown condition agrees with (21), because for the map (19) we have

$$z_M^{\inf} := \inf_{\theta \in [0, 2\pi)} \left[\psi_M(e^{i\theta}) \right] = \psi_M(1) = \frac{1}{(\sqrt{2} + 1)^{2/M}}.$$
 (31)

Therefore

$$N_c^{\inf}(M) = \frac{-M \log_{10}(\epsilon)}{4 \log_{10}(\sqrt{2} + 1)}$$
(32)

in agreement with (20).

5. Physical applications

In nontrivial applications we typically do not know the full Riemann surface structure of the function being approximated. However, in many physical and mathematical applications the function's behavior is dominated by finitely many singularities, often just one or two. In such situations, even approximate information about these dominant singularities can be used to construct accurate approximations to the function that are significantly more precise than the original series expansion.

But now we ask what happens in the presence of noise. Our main result is that the key quantity in relating the number of terms at which Padé breaks down to the strength of the noise is the conformal map produced by Padé in the large N limit. Importantly for applications, this map only depends on the *locations* of the singularities, so the relation between N_c and the noise strength can be estimated using even approximate information about the singularity locations.

To illustrate the generality of this result, we now study the numerical analysis of two non-trivial examples coming from physical and mathematical applications, where we do not know the exact conformal map, but we can construct an approximate map based on the *leading* singularities. These are applications in which it is possible to generate terms of an asymptotic expansion, with *exact* rational coefficients, and the divergent formal series can be used to explore the singularity structure of the corresponding Borel plane using combinations of Padé approximants and conformal and uniformizing maps. But in both cases, the Borel plane has an intricate multi-sheeted Riemann surface structure, so the underlying functions are much more complicated than the simple one-cut and two-cut functions used in the numerical experiments in sections 2.1 and 2.2. Nevertheless, we show that estimates based on their leading singularities match very closely the actual behavior of Padé in the presence of noise.

5.1. Renormalization in quantum field theory

Perturbation theory in quantum mechanics and quantum field theory (QFT) is generically divergent, with factorially growing coefficients [18]. In QFT it is generally difficult to generate many terms of a perturbative expansion, and frequently such an expansion has coefficients that are only approximate. In this section we choose a particular computation of the anomalous dimension $\gamma(a)$ in an asymptotically free conformal theory, scalar φ^3 theory in 6 dimensional spacetime. This is a well-studied theory [27–31], and one for which high orders of perturbation theory are accessible using the Kreimer–Connes Hopf algebraic approach to renormalization [32]. Broadhurst and Kreimer showed that in this approach the perturbative expansion of the anomalous dimension $\gamma(a)$ is characterized by a quartically nonlinear third order ordinary differential equation (ODE) for $\gamma(a)$ [33]. The resurgent trans-series structure of this function has recently been analyzed in detail in [34, 35], revealing an intricate Borel Riemann surface structure. On the first sheet there is a single *dominant* Borel branch point singularity with exponent $\frac{1}{12}$, in addition to two further resonant collinear Borel singularities, and all three of these singularities are repeated in integer multiples. Here we show that if noise is introduced to this computation, the result is dominated by the leading Borel singularity, so

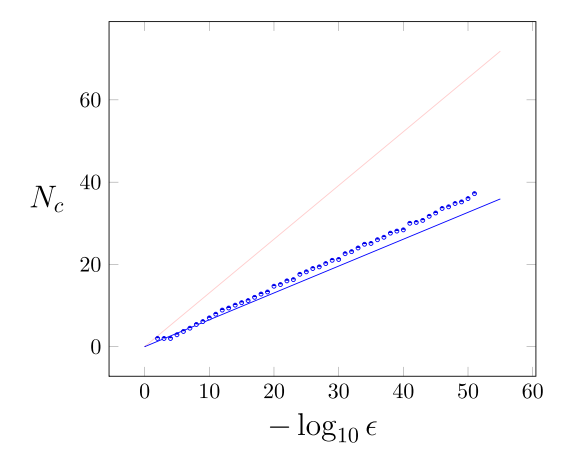


Figure 9. This plot shows the critical truncation order N_c at which Padé breaks down in the presence of noise, as a function of the logarithm of the noise strength, for the Borel transform (33) of the anomalous dimension in the Hopf algebraic analysis of the φ^3 scalar quantum field theory in 6 dimensions [33, 34]. The blue dots show the average of multiple realizations of the random noise, and the blue line shows the general one-cut scaling relation in (18). Contrast this with the faint red line which shows the slope for the two-cut case.

the slope relating the breakdown order N_c to the logarithm of the noise strength, as in (30), can be well approximated by the one-cut situation.

The function under consideration is the Borel transform (see equation (29) in [34])

$$G(\omega) = 6\sum_{n=0}^{\infty} (-1)^n \frac{A_n}{12^n} \frac{\omega^n}{n!}$$
 (33)

where the coefficients A_n appear as A051862 in the Online Encyclopedia of Integer Sequences. Truncating this expansion at a given order, we can apply Padé to analytically continue the Borel transform, in order to obtain a resummation of the divergent perturbative expansion of the anomalous dimension. If we then introduce noise to the expansion coefficients, as in (4), then we observe that the Padé approximation to $G_{\epsilon}(\omega)$ breaks down at a truncation order N_c that depends on the strength of the noise. Figure 9 plots this critical truncation order N_c as a function of the logarithm of the noise. It is quite remarkable that such a drastic approximation of only considering the effect of the location of a single *dominant* branch point singularity captures the general trend quite accurately.

5.2. Tritronquée solution to Painlevé I

The Painlevé equations generate solutions known as the 'nonlinear special functions', with a wide range of applications in physics and in mathematics [36]. Asymptotic expansions of these functions can be described in terms of resurgent trans series [37], and their Borel transforms have a rich Riemann surface structure, with infinitely many sheets [23]. As a concrete example we consider the Borel transform of the perturbative expansion of the tritronquée solution to Painlevé I, which arises in physical applications in matrix models of 2d gravity [38]. This special solution F(x) undergoes nonlinear Stokes transitions in the physical domain when Arg(x) is an integer multiple of $\frac{2\pi}{5}$. In the Borel plane the tritronquée Borel transform function $f(\omega)$

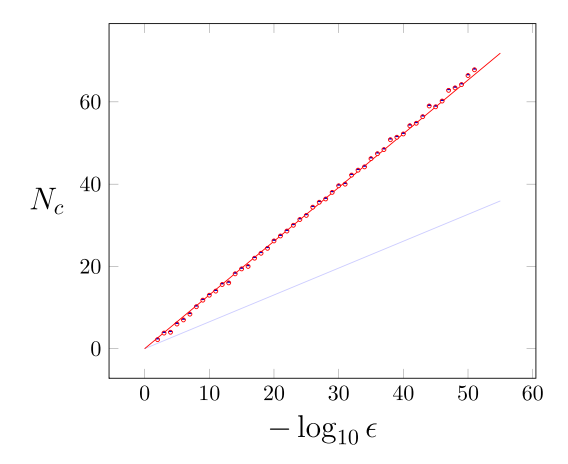


Figure 10. This plot shows (red dots) the critical truncation order N_c at which Padé breaks down in the presence of noise, as a function of the logarithm of the noise strength, for the Borel transform (34) of the tritronquée solution of the Painlevé I equation [39]. The red dots show the average of multiple realizations of the random noise, and the red line shows the general two-cut scaling relation in (20) with M = 2. The faint blue line shows the slope for the one-cut scaling relation, for contrast.

has two infinite towers of collinear Borel singularities, at all integer multiples of a \pm pair. The analysis of [39] shows that this solution can be accurately analytically continued into the complex x plane, starting from an asymptotic expansion generated for $x \to +\infty$, even crossing into the Dubrovin pole region $\frac{4\pi}{5} < \text{Arg}(x) < \frac{6\pi}{5}$ [40, 41]. The Borel transform can be defined as [39]

$$B(\omega) = \sum_{n=1}^{\infty} \frac{a_n}{(2n-1)!} \,\omega^{2n-1}.\tag{34}$$

The expansion coefficients a_n are rational numbers, generated from the recursion relation

$$a_{n} = -4(n-1)^{2} a_{n-1} - \frac{1}{2} \sum_{m=2}^{n-2} a_{m} a_{n-m} , \quad n \geqslant 3$$

$$a_{1} = \frac{4}{25} , \quad a_{2} = -\frac{392}{625}.$$
(35)

In the absence of noise, finite-order truncations of this Borel transform encode non-trivial information about the global analytic properties of the tritronquée solution [39]. When we introduce noise, as in (4), Padé approximation to $B_{\epsilon}(\omega)$ breaks down at a truncation order N_c that depends on the strength of the noise. Figure 10 plots this critical truncation order N_c as a function of the logarithm of the noise. Once again we see that consideration of the effect of the dominant pair of branch point Borel singularities is sufficiently accurate to describe the effect of noise on this expansion.

6. Conclusions

We have analyzed the effect of noise on Padé approximants, for functions with general branch point singularities of the form that arise in a broad class of physical applications. With noisy input coefficients, the Padé approximant breaks down at a certain Padé order, N_c, which is proportional to the log of the noise strength. Furthermore, the proportionality constant can be expressed in terms of the conformal map that Padé generates in its large order limit. We have presented two natural ways to characterize the breakdown of Padé: one based on a sudden change in the distribution of the Padé poles, and another based on a change in the relative precision of the Padé approximant. Our main results are theorem 4.4 and corollary 4.5, which characterize the breakdown condition both globally and locally. For a given level of noise there is an order beyond which Padé will begin to introduce spurious poles that do not represent the true singularity structure of the function being approximated. Correspondingly, the extrapolation accuracy of Padé will degrade beyond this threshold breakdown order. Theorem 4.4 and corollary 4.5 furthermore identify the locations at which spurious poles form. The proportionality constant relating the breakdown order to the logarithm of the noise strength can be expressed in terms of the conformal map that Padé generates at large order. Therefore this slope can be estimated just based on the locations of the singularities, not requiring full information about the function itself. Furthermore, we have shown that in some non-trivial problems the slope can be accurately estimated based solely on the effect of the *dominant* singularities, not even requiring knowledge of the exact conformal map. We anticipate that this result can have implications in a wide range of physical applications. An important open question is to determine optimal strategies for extrapolation in the presence of noisy coefficients, generalizing the results of [23] for the noise-free case.

Data availability statement

The data that support the findings of this study are available upon reasonable request from the authors.

Acknowledgments

This work is supported in part by the U.S. Department of Energy, Office of High Energy Physics, Award DE-SC0010339 (GD, MM), and by the U.S. National Science Foundation, Division of Mathematical Sciences, Award NSF DMS—2206241 (OC).

ORCID iD

Gerald V Dunne https://orcid.org/0000-0003-1338-339X

References

- Baker G A and Graves-Morris P 2009 Padé Approximants (Cambridge: Cambridge University Press)
- [2] Bender C M and Orzsag S A 1999 Advanced Mathematical Methods for Scientists and Engineers (Berlin: Springer)
- [3] Stahl H 1997 The convergence of Padé approximants to functions with branch points *J. Approx. Theory* **91** 139–204
- [4] Saff E B 2010 Logarithmic potential theory with applications to approximation theory Surv. Approx. Theory 5 165–200
- [5] Gonchar A A, Rakhmanov E A and Suetin S P 2011 Padé-Chebyshev approximants of multivalued analytic functions, variation of equilibrium energy and the S-property of stationary compact sets Russ. Math. Surv. 66 1015–48

- [6] Aptekarev A I, Buslaev V I, Martínez-Finkelshtein A and Suetin S P 2011 Padé approximants, continued fractions and orthogonal polynomials Russ. Math. Surv. 66 1049–131
- [7] Martínez-Finkelshtein A, Rakhmanov E A and Suetin S P 2012 Heine, Hilbert, Pade, Riemann and Stieltjes: John Nuttall's work 25 years later Contemp. Math. 578 165–93
- [8] Aptekarev A and Yattselev M L 2015 Padé approximants for functions with branch points—strong asymptotics of Nuttall-Stahl polynomials Acta Math. 215 217–80
- [9] Costin O and Dunne G V 2021 Conformal and uniformizing maps in Borel analysis Eur. Phys. J. Spec. Top. 230 2679–90
- [10] Froissart M 1969 Approximation de Padé. Application à la physique des particules elémentaires Les Rencontres Physiciens-Mathématiciens de Strasbourg RCP25 9 1–13
- [11] Bessis D 1996 Padé approximations in noise filtering J. Comput. Appl. Math. 66 85–88
- [12] Bessis D and Perotti L 2009 Universal analytic properties of noise: introducing the J-matrix formalism J. Phys. A: Math. Theor. 42 365202
- [13] Gilewicz J and Pindor M 1997 Padé approximants and noise: a case of geometric series J. Comput. Appl. Math. 87 199–214 Gilewicz J and Pindor M 1999 Padé approximants and noise: rational functions J. Comput. Appl. Math. 105 285–97
- [14] Gilewicz J and Kryakin Y 2003 Froissart doublets in Padé approximation in the case of polynomial noise J. Comput. Appl. Math. 153 235–42
- [15] Zinn-Justin J 2002 Quantum Field Theory and Critical Phenomena (International Series of Monographs on Physics) vol 113 (Oxford: Oxford University Press) p 1
- [16] Costin O and Dunne G V 2020 Physical resurgent extrapolation *Phys. Lett.* B 808 135627
- [17] Yamada H S and Ikeda K S 2013 A numerical test of Padé approximation for some functions with singularity (arXiv:1308.4453)
- [18] Guillou J C L and Zinn-Justin J (ed) 1990 Large Order Behavior of Perturbation Theory (Amsterdam: North-Holland)
- [19] Kuz'mina G V 1969 Estimates for the transfinite diameter of a family of continua and covering theorems for univalent functions *Proc. Steklov Inst. Math.* 94 53–74
- [20] Grassmann E G and Rokne J 1975 An explicit calculation of some sets of minimal capacity SIAM J. Math. Anal. 6 242–9
- [21] Ransford T 2011 Computation of logarithmic capacity Comput. Methods Funct. Theory 10 555-78
- [22] Damanik D and Simon B 2006 Jost functions and Jost solutions for Jacobi matrices, I. A necessary and sufficient condition for Szegö asymptotics *Invent. Math.* 165 1–50
- [23] Costin O and Dunne G V 2022 Uniformization and constructive analytic continuation of Taylor series Commun. Math. Phys. 392 863–906
- [24] Brown J W and Churchill R V 2009 Complex Variables and Applications 8th edn (New York: McGraw-Hill)
- [25] Kober H 1957 Dictionary of Conformal Representations (New York: Dover)
- [26] Kahane J-P 1985 Some Random Series of Functions (Cambridge Studies in Advanced Mathematics Vol 5) 2nd edn (Cambridge: Cambridge University Press)
- [27] Lipatov L N 1977 Divergence of the perturbation theory series and the quasiclassical theory Sov. Phys. JETP 45 216–23
- [28] Fisher M E 1978 Yang-Lee edge singularity and ϕ^3 field theory *Phys. Rev. Lett.* **40** 1610–3
- [29] McKane A J 1979 Vacuum instability in scalar field theories Nucl. Phys. B 152 166–88
- [30] de Alcantara Bonfim O F, Kirkham J E and McKane A J 1981 Critical exponents for the percolation problem and the Yang-Lee edge singularity J. Phys. A 14 2391
- [31] Borinsky M, Gracey J A, Kompaniets M V and Schnetz O 2021 Five-loop renormalization of φ^3 theory with applications to the Lee-Yang edge singularity and percolation theory *Phys. Rev.* D 103 116024
- [32] Connes A and Kreimer D 2000 Renormalization in quantum field theory and the Riemann-Hilbert problem. 1. The Hopf algebra structure of graphs and the main theorem *Commun. Math. Phys.* 210 249–73 Connes A and Kreimer D 2001 Renormalization in quantum field theory and the Riemann-Hilbert problem. 2. The beta function, diffeomorphisms and the renormalization group *Commun. Math. Phys.* 216 215–41
- [33] Broadhurst D J and Kreimer D 2000 Combinatoric explosion of renormalization tamed by Hopf algebra: thirty loop Pade-Borel resummation *Phys. Lett.* B 475 63–70 Broadhurst D J and Kreimer D 2001 Exact solutions of Dyson-Schwinger equations for iterated one loop integrals and propagator coupling duality *Nucl. Phys.* B 600 403–22

- [34] Borinsky M, Dunne G V and Meynig M 2021 Semiclassical trans-series from the perturbative Hopf-Algebraic Dyson-Schwinger equations: φ^3 QFT in 6 dimensions SIGMA 17 087
- [35] Borinsky M and Broadhurst D J 2022 Resonant resurgent asymptotics from quantum field theory Nucl. Phys. B 981 115861
- [36] Clarkson P A 2006 Painlevé equations—nonlinear special functions Orthogonal Polynomials and Special Functions (Lecture Notes in Mathematics) vol 1883, ed F Marcellán and W Van Assche (Berlin: Springer)
- [37] Costin O 2008 Asymptotics and Borel Summability (Boca Raton, FL: Chapman and Hall/CRC)
- [38] Di Francesco P, Ginsparg P H and Zinn-Justin J 1995 2-D gravity and random matrices Phys. Rep. 254 1–133
- [39] Costin O and Dunne G V 2019 Resurgent extrapolation: rebuilding a function from asymptotic data. Painlevé I J. Phys. A 52 445205
- [40] Dubrovin B, Grava T and Klein C 2009 On universality of critical behavior in the focusing nonlinear Schrödinger equation, elliptic umbilic catastrophe and the tritronquée solution to the Painlevé-I equation J. Nonlinear Sci. 19 57–94
- [41] Costin O, Huang M and Tanveer S 2014 Proof of the Dubrovin conjecture and analysis of the tritronquée solutions of PI Duke Math. J. 163 665–704